

Coronal and chromospheric emission in A-type stars

HANS MORITZ GÜNTHER,¹ CARL MELIS,² J. ROBRADÉ,³ P. C. SCHNEIDER,³ SCOTT J. WOLK,⁴ AND RAKESH K. YADAV⁵

¹MIT Kavli Institute for Astrophysics and Space Research, 77 Massachusetts Avenue, Cambridge, MA 02139, USA

²Center for Astrophysics and Space Sciences, University of California, San Diego, CA 92093-0424, USA

³Hamburger Sternwarte, Gojenbergsweg 112, 21029 Hamburg, Germany

⁴Smithsonian Astrophysical Observatory, MS 70, 60 Garden St., Cambridge, MA 02138

⁵Department of Earth and Planetary Sciences, Harvard University, Cambridge, MA 02138, USA

ABSTRACT

Cool stars on the main sequence generate X-rays from coronal activity, powered by a convective dynamo. With increasing temperature, the convective envelope becomes smaller and X-ray emission fainter. We present Chandra/HRC-I observations of four single stars with early A spectral types. Only the coolest star of this sample, τ^3 Eri ($T_{\text{eff}} \approx 8,000$ K), is detected with $\log(L_X/L_{\text{bol}}) = -7.6$ while the three hotter stars ($T_{\text{eff}} \geq 8,000$ K), namely δ Leo, β Leo, and ι Cen, remain undetected with upper limits $\log(L_X/L_{\text{bol}}) < -8.4$. The drop in X-ray emission thus occurs in a narrow range of effective temperatures around ~ 8100 K and matches the drop of activity in the C III and O VI transition region lines.

1. INTRODUCTION

Stars across the main-sequence (MS) produce X-ray emission in two fundamentally different mechanisms. Cool stars have convective envelopes, which can produce differential rotation and convective turbulence, giving rise to strong magnetic fields through the dynamo mechanism (Brun & Browning 2017). These magnetic fields then help sustain coronal activity around these stars. Essentially all close-by late-type stars are X-ray emitters (Schmitt & Liefke 2004). On the other end of the MS the most massive stars have fast winds. Instabilities in the winds heat the gas to a few MK. Again, nearly all of them are X-ray emitters (Berghoefer et al. 1996, 1997). Stars from mid-A to B operate neither mechanism: Their winds are too weak to produce detectable X-ray emission and their atmospheres are radiatively dominated and do not drive a turbulent convective dynamo. Mid-A to B-type stars thus are X-ray dark (Schmitt 1997).

Nevertheless, some A and B-type stars are seen in the ROSAT All-Sky Survey (RASS) or in other X-ray datasets (Wang et al. 2020), because they often have unresolved late-type companions. Due to the shorter lifetime of the A-type star, the companion is still at an early stage of its evolution when the A-star is on the MS and thus the companion is X-ray bright. The RASS catalog contains 312 bright A-type stars. This is a detection rate of 10-15% (Schröder & Schmitt 2007). In the sub-sample studied by Huélamo et al. (2000), X-ray hardness and flux are similar to late-type stars indicat-

ing unresolved companions are responsible for that emission. Stelzer et al. (2003) observed five RASS sources with apparent X-rays with Chandra. In three targets the X-rays are due to a resolved companion, and Stelzer et al. (2003) argue based on spectral properties that the remaining targets probably have an unresolved companion that generates the X-ray emission.

However, star spots leading to photometric variability with a low amplitude of 0.05% have been found for Vega (Böhm et al. 2015) together with a weak (disk-averaged line-of-sight component < 1 G) magnetic field (Lignières et al. 2009; Petit et al. 2010). Also, recent studies with Kepler and TESS do indeed find rotational modulation of early A-type stars (Balona 2011, 2017; Sikora et al. 2019) and sometimes signatures of what seem to be magnetic flares (Balona 2012). However, the latter can usually be attributed to binarity or artifacts such as contamination of the lightcurve by nearby sources (Pedersen et al. 2017).

Simon et al. (2002) and Neff & Simon (2008) systematically observed mid-A type stars in the ultraviolet (UV) looking for the subcoronal emission lines of C III and O VI formed between 50,000 and 300,000 K (Dere et al. 1997; Del Zanna et al. 2021). They find a very sharp cut-off, where stars with $T_{\text{eff}} < 8200$ K have line fluxes similar to our Sun (Ayres 1997) when normalized to the bolometric luminosity, but they claim these lines are undetected in stars with $T_{\text{eff}} > 8300$ K. The exact numbers given for T_{eff} depend on the effective temperature scale adopted, and will be slightly different in this work. Simon et al.

(2002) conclude that the transition between stars with and without a corona happens within 100 K and that the cut-off temperature is compatible with theoretical predictions (Christensen-Dalsgaard 2000; Kupka & Montgomery 2002). Neff & Simon (2008) observed O VI in 6 of 8 stars with $T_{\text{eff}} > 8300$ K, but similar to the X-rays, then present several lines of evidence that the X-ray emission is due to a low-mass companion in all six cases.

Simon et al. (2002) also analyzed archival *ROSAT* observations and find X-ray emission only for stars that appear below 8200 K on their temperature scale. However, the X-ray sensitivity was not very high by modern standards. In this paper, we present new *Chandra*/HRC-I observations that are about an order of magnitude more sensitive for the stars in the Simon et al. (2002) sample that previously only had *ROSAT* data. To avoid the problem of unresolved companions, we limit the new observations to well-studied A stars within 30 pc where spectroscopy and recent planet searches with the radial-velocity method (e.g. Hurt et al. 2021), direct imaging (e.g. Nielsen et al. 2013; Meshkat et al. 2017), and the study of anomalous GAIA proper motion (Kervella et al. 2019) essentially rule out the presence of a late-type stellar companion, i.e., our target sample comprises only bona fide single stars.

There are two special classes of A-type stars where X-ray emission is commonly observed: (1) Chemically peculiar Ap (Babel & Montmerle 1997; Robrade & Schmitt 2011) stars have magnetic fields presumably strong enough to funnel their stellar wind into the equatorial plane where shocks develop, and (2) pre-main sequence stars (Herbig Ae stars, e.g. Skinner et al. 2004; Skinner & Güdel 2020; Telleschi et al. 2007; Günther & Schmitt 2009), some of which even show magnetically collimated jets. Both classes are markedly different in magnetic properties and power sources available for X-ray generation and are not considered any further in this study.

In section 2, we show the data from those new observations. We discuss the results in section 3 and summarize our findings in section 4.

2. DATA ANALYSIS

We observed four A-types stars with *Chandra*/HRC-I. Details of the observations are listed in Table 1. Data was reprocessed with CIAO 4.13 (Fruscione et al. 2006), following standard analysis procedures. For reproducibility, we provide the full analysis script¹.

First, we try to improve the astrometry of the *Chandra* observations. The 90% uncertainty circle for *Chandra* absolute astrometry is $0.8''^2$. Since the relative precision is even better than that, the astrometry can be improved if a sufficient number of sources can be matched to a catalog with high astrometric precision. We run the CIAO task `wavdetect` on the X-ray data to detect X-ray sources with the intent to cross-match them with 2MASS (Skrutskie et al. 2006) or GAIA (Gaia Collaboration et al. 2016, 2018). In ObsID 18933, we find 2MASS J03021318-2335198, a Seyfert 1 galaxy, to be located 0.7 arcsec to the East of the peak of the X-ray emission; in all other cases we do not find reliable, unambiguous matches or the matched sources are located so far from the aimpoint that their point-spread-function (PSF) is too large to improve coordinate accuracy.

Figure 1 shows the *Chandra*/HRC-I images of our four targets. A circle with 1 arcsec radius marks the position of the target at the time of the observation. Coordinates and proper motions are taken from Gaia Collaboration (2018) for ι Cen and from van Leeuwen (2007) for the remaining three targets. Only τ^3 Eri has significant emission within the marked circle in Fig. 1. The expected position is about 0.7 arcsec to the East of the peak of the X-ray emission; the direction and distance of the offset are very similar to the offset detected in 2MASS J03021318-2335198 and within the 90% uncertainty expected for the *Chandra* coordinates. We thus conclude that the apparent distance is in fact due to the uncertainties of the *Chandra* coordinates and that the source seen is a detection of τ^3 Eri.

Next, we determine source flux and uncertainties or upper limits. We chose a source extraction region with 1.5 arcsec radius to ensure that the source flux is captured even in the presence of coordinate uncertainties. The *Chandra* PSF depends on the photon energy, but for soft sources as expected here, that region captures well above 95% of the PSF. Without knowing the source spectrum, we cannot fully correct for the loss of photons outside the source aperture. The background flux is determined from a large region that is apparently source-free; in this way the statistical error on the background rate is small.

For τ^3 Eri, we calculate 90% credible intervals on the X-ray flux following a Bayesian approach that takes into account the presence of a background (Primini & Kashyap 2014) as implemented in the CIAO tool `aprates`. For the three undetected sources, we calculate upper limits following the procedure of Kashyap

¹ <https://github.com/hamogu/HottestCoolStar/blob/main/figures/HottestCoolStar.ipynb>

² <https://cxc.cfa.harvard.edu/cal/ASPECT/celmon/>

Table 1. Chandra observations with pointing information

target	obs. date	OBSID	RA (pointing) °	Dec (pointing) °	exp. time ks
ι Cen	2017-03-31	18930	200.1525	-36.7119	9.7
β Leo	2017-04-05	18931	177.2635	14.5719	10.1
δ Leo	2017-02-05	18932	168.5285	20.5240	10.1
τ^3 Eri	2017-06-09	18933	45.5957	-23.6223	19.9

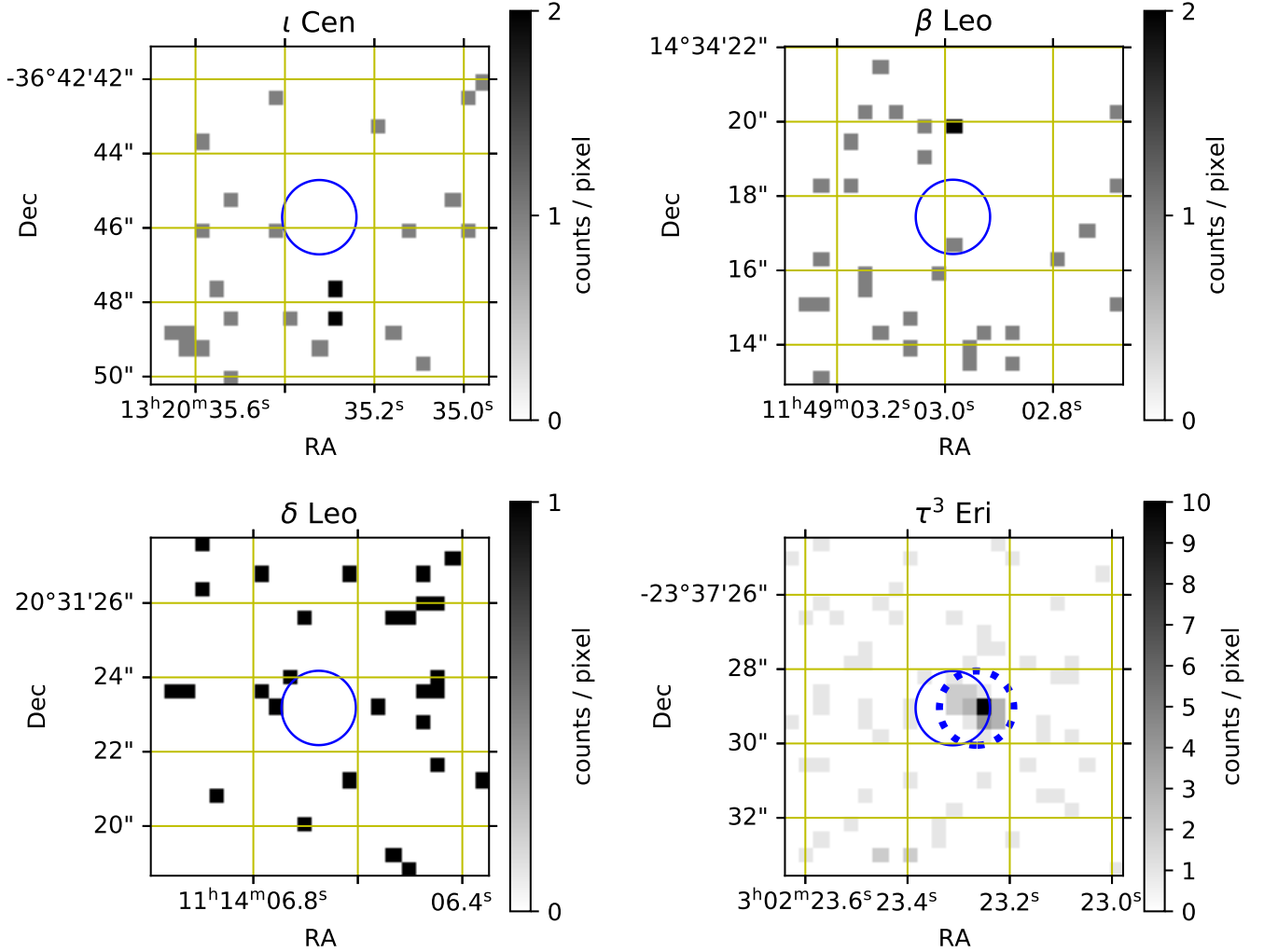


Figure 1. Observations with the Chandra/HRC. The blue circles mark a 1 arcsec radius around the expected position of the target accounting for proper motion at the time of the observation. For τ^3 Eri, the dotted circle accounts for the coordinate offset discussed in the text.

et al. (2010). Deriving an upper limit requires the choice of two parameters. We set the probability of a “false positive” (a background fluctuation that is erroneously detected as a source) to be $< 0.3\%$ corresponding to a Gaussian-equivalent of “ 3σ ” and the probability of a “false negative” (a real source with a true flux above the given upper limit that is not detected because, due to drawing by chance from a Poisson distribution, the

number of photons in the observation is so low that it is compatible with background) to be $< 50\%$.

Table 2 lists the detected count rate or upper limit. We convert the count rate into an energy flux, assuming a thermal spectrum. For Chandra/HRC-I, 1 ct ks^{-1} corresponds to an X-ray flux about 1.0×10^{-14} erg s^{-1}

in the 0.1-5 keV band according to WebPIMMS³; the variation around this value is no more than 15% in the temperature range 0.8-13 MK. Using the distance and bolometric luminosity from Simon et al. (2002), Table 2 also lists L_X and $\log(L_X/L_{\text{bol}})$.

All target stars are optically bright. We compare their V magnitude to Vega and scale the number of observed UV events from observations of Vega (Pease et al. 2006). Based on this we expect 1 or fewer UV events for each observation and we conclude that UV contamination is negligible. For τ^3 Eri, we checked the lightcurve and we do not find any significant variability, but –given the low-count number– even a flare that doubles the X-ray output for a few ks could be hidden in the Poisson noise.

3. RESULTS AND DISCUSSION

Our Chandra observations followed up on four targets where Simon et al. (2002) could only give upper limits from *ROSAT* data. We detected τ^3 Eri and pushed the upper limit on L_X for δ Leo, β Leo, and ι Cen down by about an order of magnitude (Table 2). With that, there is now a one-to-one correspondence between X-ray emission and the transition region lines C III and O VI which are formed between 50,000 and 300,000 K from the sample of Simon et al. (2002). X-ray and C III 977 Å fluxes are listed in Table 3, which also includes a comparison fluxes and upper limits to other main-sequence stars from the literature. In the following, discuss implications in the light of other observational or theoretical work that has become available since the Simon et al. (2002) data were published.

Note that ages given in Table 3 are often based on membership in moving groups. In some cases, membership is under debate and stars could be considerably older if they turn out to be field stars, e.g., see the discussion and references in Defrère et al. (2021) for β Leo. Table 3 also gives an effective temperature for the stars. No single survey covers all stars in Table 3 and it is well known that different classification methods lead to discrepant spectral types (e.g., Gray & Garrison 1989). Additionally, the stellar surface of A-type stars is not necessarily well described by a single spectral type or temperature; e.g. Robrade & Schmitt (2010) argued that the spectral classification of HR 8799 of A5 is based on metal lines, while the atmospheric temperature might be better characterized by its hydrogen lines, which would make it an F0 star (Gray & Kaye 1999), cool enough to generate magnetic activity through a convective dynamo. Similarly, Altair is a very fast rotator, and thus

it has a considerable equatorial bulge and consequently a lower temperature on the equator than on the pole, which might allow the formation of a thin convection zone in the equatorial bulge (Robrade & Schmitt 2009). The T_{eff} given in the table is the average of all values listed in the PASTEL catalog (Soubiran et al. 2016; see there for references for individual targets), which collects high precision spectroscopic and photometric measurements of the effective temperature. Where more than one measurement is available in PASTEL, the $\sigma_{T_{\text{eff}}}$ is calculated as the standard deviation of all measurements, since the systematic differences between different input data are typically larger than individual measurement uncertainties and uncertainties are not available in all cases. We stress that T_{eff} only provides an approximate measure of the photospheric temperature in the region where UV and X-rays are generated, and large temperature gradients can exist between pole and equator. Thus, the ordering in Table 3 by T_{eff} from hot to cool should be regarded as approximate.

Numbers for the rotational velocity $v \sin i$ are taken from a compilation (Royer et al. 2002), except for ι Cen which is not part of the list, so we use the value from Simon et al. (2002).

3.1. Comparing X-ray and UV fluxes

Table 3 lists one UV line, C III 977 Å, but Simon et al. (2002) show that all stars where that line can be detected also show detections in C III 1175 Å and the O VI 1032/1038 Å doublet; similarly, all stars where there is only an upper limit on C III 977 Å also only have an upper limit on the other lines. Figure 2 compares the X-ray and the C III 977 Å line fluxes as a fraction of the bolometric flux. The three X-ray undetected stars (ι Cen, δ Leo, and β Leo) are at least an order of magnitude fainter than τ^3 Eri and Alderamin, which in turn are already significantly fainter than the Sun. So, all studied A-type stars show comparatively less chromospheric and coronal activity. If this was an effect of the coronal temperature, where A-type stars have cooler coronae than the Sun, then we would expect additional emission in the UV, yet this does not seem to be the case as the C III and O VI (not shown in the figure) also drop as T_{eff} increases. The measurements instead indicate that the relative amount of emitting plasma decreases. This could mean that a lower fraction of the surface area is covered with active structures, or that those structures have lower densities or shorter lifetimes than in later-type stars.

At first sight, one might expect also a correlation with rotational velocities, where faster rotation produces a stronger X-ray activity as is clearly seen in lower mass

³ <https://heasarc.gsfc.nasa.gov/cgi-bin/Tools/w3pimms/w3pimms.pl>

Table 2. X-ray flux (90% credible interval) or upper limit (0.3% false positive and 50% false negative).

target	net. counts ct	net. rate ct ks ⁻¹	net. flux 10 ⁻¹⁵ erg s ⁻¹ cm ⁻²	L_X 10 ²⁶ erg s ⁻¹	$\log(L_X/L_{\text{bol}})$
ι Cen	0.0 .. 2.9	0.0 .. 0.3	0 .. 3	< 3.2	< -8.4
β Leo	0.0 .. 3.0	0.0 .. 0.3	0 .. 2.9	< 1.0	< -8.7
δ Leo	0.0 .. 4.8	0.0 .. 0.5	0 .. 4.7	< 2.6	< -8.5
τ^3 Eri	20.5 .. 39.8	1.0 .. 2.0	10 .. 20	6 .. 20	-7.9 .. -7.4

Table 3. Stars of spectral type A with detailed X-ray observations

name	age Myr	age ref ref	$v \sin i$ km s ⁻¹	T_{eff} K	$\sigma_{T_{\text{eff}}}$ K	C III 977 Å 10 ⁻⁷ L_{\odot}	L_X erg s ⁻¹	$\log(L_X/L_{\text{bol}})$	X-ray ref
HR 4796A	5-16	1,2,3	152	9750	113		< 1.3×10^{27}	< -7.7	16
Vega	100-500	4,5,6	25 ± 2	9372	503		< 3.0×10^{25}	< -10.0	17
ι Cen	100-400	7,8	75	9147	118	< 0.10	< 3.2×10^{26}	< -8.4	here
β Leo	30-70	9,10,11	128	8549	88	< 0.03	< 1×10^{26}	< -8.7	here
β Pic	12-40	12,13	130	8103	90		$(1.3 \pm 0.3) \times 10^{27}$	-8.2 ± 0.1	18
δ Leo	600-890	7,8	180	8076	155	< 0.04	< 2.6×10^{26}	< -8.5	here
τ^3 Eri	430-950	8	133	7999	103	0.96 ± 0.16	$12_{-6}^{+8} \times 10^{26}$	-7.6 ^{+0.2} _{-0.3}	here
Altair	700-1000	7,14	217	7651	204		$(1.4 \pm 0.2) \times 10^{27}$	-7.4 ± 0.1	19
Alderamin	1000	15	196	7438	173	1.34 ± 0.13	$(2.2 \pm 0.4) \times 10^{27}$	-7.5 ± 0.1	20
HR 8799	38-48	9	49	7187	24		$(1.3 \pm 0.2) \times 10^{28}$	-6.2 ± 0.1	21

References for column “age (ref)”: (1) Webb et al. (1999), (2) Weinberger et al. (2013), (3) Drake et al. (2014), (4) Barrado y Navascues (1998), (5) Hill et al. (2010), (6) Yoon et al. (2010), (7) Vican (2012), (8) David & Hillenbrand (2015), (9) Bell et al. (2015), (10) Zuckerman (2019), (11) Lee & Song (2019), (12) Zuckerman et al. (2001), (13) Macdonald & Mullan (2010), (14) Stone et al. (2018), (15) Zhao et al. (2009). Values for $v \sin i$ are taken from the compilation of Royer et al. (2002) (see there for references for individual targets). Only for Vega is the value for $v \sin i$ measured in that work and an uncertainty provided. ι Cen is not part of that catalog, and so the value given in Simon et al. (2002) is used instead. T_{eff} is quoted from the PASTEL catalog (Soubiran et al. 2016; see there for references for individual targets), but see Section 3 for discussion on why T_{eff} may not characterize the photospheric properties well. Fluxes and upper limits for C III 977 Å are taken from Simon et al. (2002). References for column “X-ray (ref)”: (16) Drake et al. (2014), (17) Pease et al. (2006) (18) Günther et al. (2012), (19) Robrade & Schmitt (2009), (20) Simon et al. (2002), (21) Robrade & Schmitt (2010).

main-sequence stars (Wright et al. 2011), but Table 3 does not bear that out. τ^3 Eri is seen in X-rays, while δ Leo and β Leo are equally fast rotators, but slightly hotter and not detected in X-rays. For most stars in Table 3 the rotational period is measured or can be inferred assuming that the stellar spin axis is aligned with the axis of a debris disk or planetary system. The stars not detected in X-rays are fast rotators, e.g. Vega (0.68 d, Böhm et al. 2015) and HR 4796A, (0.5 d, Drake et al. 2014), as are the stars that are detected in X-rays, e.g. Alderamin (0.5 d, van Belle et al. 2006) and Altair (0.4 d, Peterson et al. 2006). Thus, the deciding factor for detectability of X-ray and transition region UV is not the rotation period, but seems to be the spectral type or photospheric temperature.

3.2. Comparison with earlier and later stars

Figure 3 compares A stars from Table 3 with earlier and later-type stars. We use the effective temperature as common axis for all datasets. O and B stars are taken

from Berghoefer et al. (1996) who distinguish between detections and upper limits. As it turns out, the upper limits are mostly in the same range of L_X/L_{bol} as the detected sources; they might just be undetected because they are further away or observed for a shorter time. To convert the spectral types of all those stars into an effective temperature, we use the compilation in Pecaut & Mamajek (2013). While that list is valid only for dwarf stars and a number of stars here have other luminosity classes, the conversion between color and temperature is sufficient for the purpose of this plot.

The X-ray activity in cool stars was studied by Wright et al. (2011). In cool stars, magnetic activity scales with Rossby number or rotation rate, so there is considerable scatter if shown as a function of effective temperature. Very few stars in the sample are listed with spectral types, so instead we use the V-K color and convert it to a temperature, again using the table from Pecaut & Mamajek (2013). We also compare the new A star

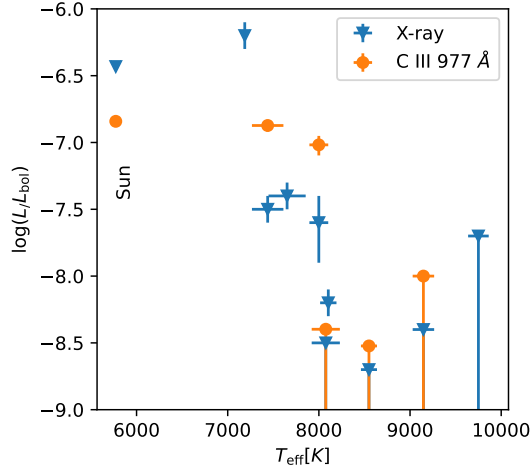


Figure 2. X-ray and C III 977 Å line flux. Both fluxes are shown relative to the star’s bolometric luminosity. Stars cooler than about 8000 K are all detected in X-rays and C III 977 Å, while stars that are significantly hotter are at least an order of magnitude fainter. The solar data is taken from (Ayres 1997), the other UV fluxes from Simon et al. (2002).

data with the stellar sources from the ROSAT survey identified by Freund (2022) who matched ROSAT and Gaia sources using a Bayesian method to select bona fide stellar X-ray sources. While their formal sample reliability is above 90% (i.e. at least 9 out of 10 sources are correctly identified as stellar), almost all companions remain unresolved in X-rays. Therefore, in many cases the ROSAT detected X-ray emission is not from the primary seen by Gaia, especially for A stars which are very often found in binary/multiple systems. This highlights that for detailed studies of A-star stellar activity, as we do in this work, it is important to select the sample carefully.

The fractional X-ray flux drops with increasing temperature for late-type stars. The brightest of the A stars (HR 8799) might follow that same trend, but the others are considerably less luminous in X-rays, indicating a qualitative change in the mechanism that generates the magnetic field and powers the X-ray emission. In particular, the early A stars (most notably Vega) have upper limits on the X-ray flux orders of magnitude below the later type stars.

Figure 3 also shows two stars with effective temperature from Berghoefer et al. (1996) very similar to our hottest stars (Vega and HR 4796A) in effective temperature, but as bright in X-rays as typical later type stars or the brightest B-type stars. However, HR 5413 (HIP 70931) has a low-mass companion ($0.23 M_{\odot}$) at 0.6 arcsec resolved with adaptive optics imaging (De Rosa et al. 2014) which might well be the X-ray source and for

HR 5846 (HIP 77086) a low-mass companion is indicated by a Gaia proper-motion anomaly (Kervella et al. 2019). The mass estimate for the companion depends on the orbital separation, but this might well be an X-ray active low-mass star. These two examples demonstrate why a study of A-star X-ray activity requires a sample of well studied targets with strict limits on binarity.

3.3. Coronal and chromospheric activity

Simon et al. (2002) detect the UV emission lines of C III at 977Å and 1175Å as well as the O VI doublet 1032/1037Å in single stars up to spectral type A4 (which they associate with $T_{\text{eff}} = 8200$ K), but not in hotter stars. They also see those lines in β Ari, which has a primary component hotter than this limit, but conclude that the most likely origin for the observed emission is chromospheric activity in the cooler secondary in the system. The emission lines of C III and O VI are formed below the corona; they have peak formation temperatures between 50,000 K and 300,000 K. Combining our new, more sensitive Chandra data with the X-ray data already discussed in Simon et al. (2002), we now see a one-to-one correspondence between X-ray emission and C III and O VI lines in the single stars. This confirms that corona and chromosphere are powered by the same mechanism. As stars become hotter, the convective envelope shrinks and at some point the dynamo mechanism breaks down.

Within the uncertainties τ^3 Eri, β Pic, and β Leo could have the same T_{eff} , yet the latter is undetected in X-rays with an upper limit a few times below the L_X/L_{bol} and $L_{\text{CIII}}/L_{\text{bol}}$ (Figure 2) for τ^3 Eri and β Pic. This indicates that the drop in X-ray and UV activity is very sharp and occurs within $\Delta T_{\text{eff}} < 200$ K. The exact boundary could depend on other factors, such as age or metallicity, which would have to be probed by a larger sample.

3.4. A-star X-ray emission: Debris disks, planets, or spectral type?

Debris disks have been found in HR 4796A (e.g. Jura 1991), Vega (e.g. Su et al. 2005), ι Cen (e.g. Quanz et al. 2011), β Leo (e.g. Defrère et al. 2021), and β Pic (e.g. Larwood & Kalas 2001). These debris disks form when planets or planetesimals in orbit around the star collide. The smaller dust grains are blown out of the system through radiation pressure relatively quickly and need to be replenished constantly by grinding down larger objects. Some stars with debris disks have X-ray and transition region UV emission, others do not, so we conclude that the presence of debris disks is not the deciding factor for chromospheric or coronal activity.

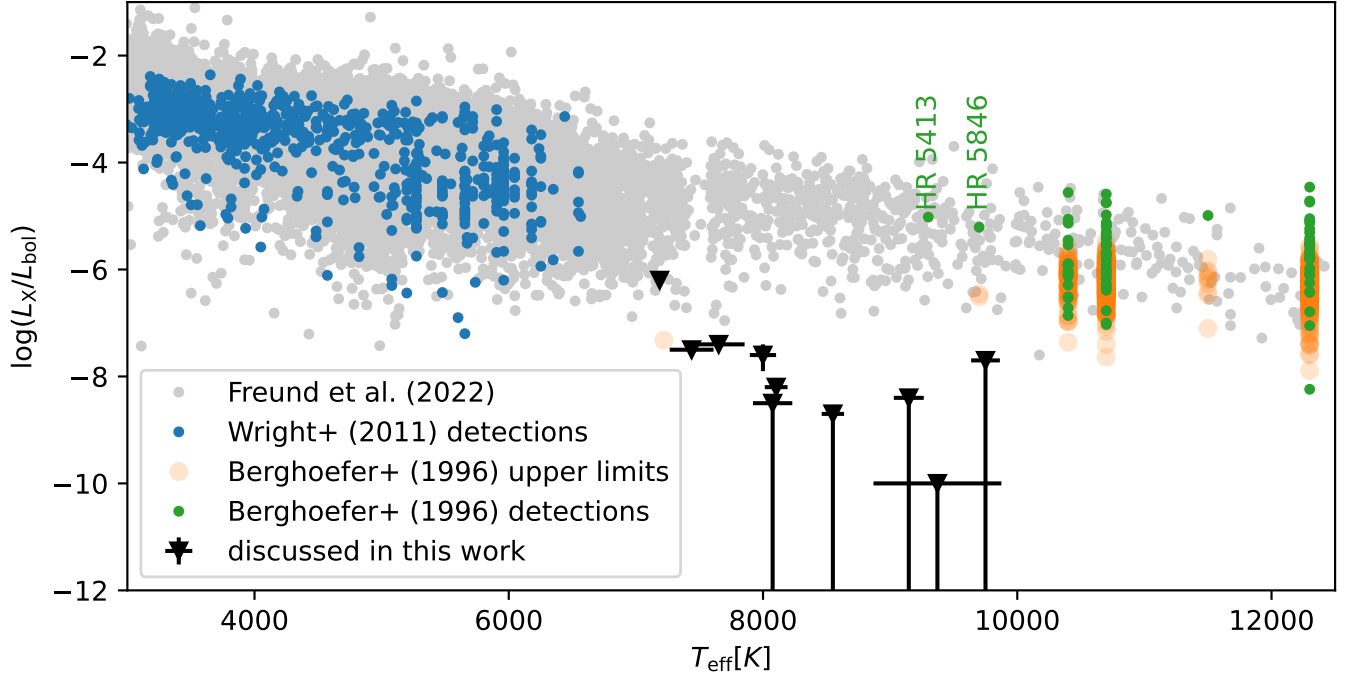


Figure 3. Comparison of the X-ray luminosity in A-type stars with data for earlier and later spectral types. Early A-type stars are fainter in X-rays than other spectral types. Note that the ROSAT catalog compiled by Freund (2022) does not resolve most binaries and thus especially the data points listed in the range $T_{\text{eff}} = 7500 - 10000$ K represent the L_{bol} from an A-star primary and the L_X from an unresolved late-type companion. This highlights the importance of carefully selecting a sample of single A stars as done in this work (black points).

Since they are close and bright targets, the stars in Table 3 have also been targeted by planet searches. Massive planets are confirmed for HR 8799 (Marois et al. 2008) and β Pic (e.g. Brandt et al. 2021), but they are located at several AU distance from the star and are thus unlikely to influence the X-ray emission from the star.

For late-type stars with a convective dynamo, X-ray activity can be parameterized by the Rossby number, or the ratio of the rotation period P_{rot} to the convective turnover time τ_{conv} , i.e.

$$\text{Ro} \sim \frac{P_{\text{rot}}}{\tau_{\text{conv}}}. \quad (1)$$

A higher Rossby number is associated with lower X-ray activity across pre-main sequence, main sequence, and giant stars (Preibisch & Feigelson 2005; Pizzolato et al. 2003; Gondoin 2005; Wright et al. 2011) and established in stellar dynamo models (e.g. Brandenburg & Schmitt 1998).

Given that many stars in Table 3 have rotation periods less than a day, the decline of the X-ray emission, and thus (in the scheme of a solar-like dynamo) increasing Rossby number, then points to a rapidly declining τ_{conv} with increasing photospheric temperature.

3.5. How could a dynamo operate in A-type stars?

X-ray activity is common in later-type stars and for Altair Robrade & Schmitt (2009) concluded that the X-ray activity is probably concentrated in the equatorial region, which is also responsible for the generation of the chromosphere (Ferrero et al. 1995). Similar to Altair, τ^3 Eri is also a rapid rotator with $v \sin i = 180 \text{ km s}^{-1}$ and an estimated oblateness (depending on the inclination angle i) of around 7% (van Belle 2012). On the other hand, δ Leo is an equally fast rotator and remains undetected.

Cantiello & Braithwaite (2019) suggest the presence of convection zones in A and late B stars very close to the surface. These thin zones are caused by partial ionization of H and He. For A-type stars about $10^{-2} - 10^{-3}$ of the total L_{bol} is transported through convective motion. Assuming equipartition between kinetic and magnetic energy, only 10^{-4} of the available magnetic energy would have to be converted into X-ray flux to power the observed X-ray luminosity. However, since the structure of those fields would differ markedly from the Sun, coronal heating would also look very different. Furthermore, Cantiello & Braithwaite (2019) predict that this mechanism should operate to mid-B type stars, in contrast

to the drop of L_X/L_{bol} that we observe in mid-A type stars in our sample.

Drake et al. (2014) extensively discuss two types of shear dynamos that could transform some initial differential rotation of a young star into a magnetic field that quickly decays, on time scales of order of a Myr for a dynamo based on magnetic buoyancy (Tout & Pringle 1995) or on times scales of order 300 yr for a dynamo based on the Taylor instability (Spruit 2002; Braithwaite 2006). Both scenarios involve physical parameters that are uncertain by orders of magnitude and Drake et al. (2014) use their upper limit on the X-ray flux from HR 4796A to exclude the most optimistic values for those parameters. Our limit for β Leo is significantly stricter, but the star is also older (Table 3), which places about the same limits on the parameters for the Tout & Pringle (1995) model as does HR 4796A (See Fig 3 in Drake et al. 2014).

Rapid rotation leads to a bulged and cooler equator in these stars (on Altair Monnier et al. 2007, resolved a temperature difference between pole and equator of at least 1000 K), so one may speculate that some of the stars might be conducive to a convective instability near their equators as has been suggested by Robrade & Schmitt (2009) for Altair. If so, then a convective dynamo near the equator may sustain significant levels of magnetic activity. Since the X-ray activity is becoming appreciable starting at τ^3 Eri, it suggests that τ^3 Eri and cooler stars are in an appropriate regime to host equatorial convection.

While the X-ray emitting corona is magnetically heated, the chromosphere in late-type stars has both acoustically and magnetically heated components (Cuntz et al. 1999; Schrijver & Zwaan 2000), where the outermost and hottest layers of the chromosphere require magnetic heating (Fawzy et al. 2002). The UV lines are formed at the high end of the temperature range of the chromosphere, and thus they likely depend on magnetic heating like the corona. Our observational result that UV lines and X-rays are visible in the same objects confirms this idea.

4. SUMMARY

We present Chandra/HRC-I observations of four early A stars. τ^3 Eri is clearly detected, while we set sensitive upper limits on the other three targets. With this detection and our new upper limits that are an order of magnitude better than previous *ROSAT* data, there is now a one-to-one correspondence between X-ray emission and C III and O VI lines, which are formed between 50,000 and 300,000 K in the transition region and were observed by Simon et al. (2002). This confirms that

both regions are powered by the same physical mechanism and that this mechanism essentially switches off around $T_{\text{eff}} = 8100 \pm 200$ K as we observe a drop of X-ray luminosity by at least an order of magnitude. Given the rather old age of τ^3 Eri, which we detect in X-rays, the magnetic field that powers X-ray emission and UV lines needs to be generated continuously. We discuss different dynamo mechanisms that could power the observed X-ray emission, but we are unable to conclusively select any particular one.

This research has made use of data obtained from the Chandra Data Archive, and software provided by the Chandra X-ray Center (CXC) in the application package CIAO. This research has made use of the SIMBAD database, operated at CDS, Strasbourg, France (Wenger et al. 2000). This research has made use of the VizieR catalogue access tool, CDS, Strasbourg, France (DOI : 10.26093/cds/vizier). The original description of the VizieR service was published in Ochsenbein et al. (2000). This research has made use of NASA’s Astrophysics Data System Bibliographic Services. This publication makes use of data products from the Two Micron All Sky Survey, which is a joint project of the University of Massachusetts and the Infrared Processing and Analysis Center/California Institute of Technology, funded by the National Aeronautics and Space Administration and the National Science Foundation. This work has made use of data from the European Space Agency (ESA) mission *Gaia* (<https://www.cosmos.esa.int/gaia>), processed by the *Gaia* Data Processing and Analysis Consortium (DPAC, <https://www.cosmos.esa.int/web/gaia/dpac/consortium>). Funding for the DPAC has been provided by national institutions, in particular the institutions participating in the *Gaia* Multilateral Agreement. HMG was supported by the National Aeronautics and Space Administration through Chandra Award Number GO9-20018X issued by the Chandra X-ray Observatory Center, which is operated by the Smithsonian Astrophysical Observatory for and on behalf of the National Aeronautics Space Administration under contract NAS8-03060. C.M. acknowledges support from NASA ADAP grant 18-ADAP18-0233. S.J.W. was supported by the Chandra X-ray Observatory Center, which is operated by the Smithsonian Astrophysical Observatory for and on behalf of the National Aeronautics Space Administration under contract NAS8-03060. J.R. acknowledges support from the DLR under grant 50QR2105.

Facilities: Chandra/HRC

Software: AstroPy (Astropy Collaboration et al. 2013, 2018), astroquery (Ginsburg et al. 2019), CIAO (Fruscione et al. 2006), NumPy (Van Der Walt et al.

2011; Harris et al. 2020), Matplotlib (Hunter 2007), Sherpa (Doe et al. 2007; Burke et al. 2021)

REFERENCES

- Astropy Collaboration, Robitaille, T. P., Tollerud, E. J., et al. 2013, *A&A*, 558, A33, doi: [10.1051/0004-6361/201322068](https://doi.org/10.1051/0004-6361/201322068)
- Astropy Collaboration, Price-Whelan, A. M., Sipőcz, B. M., et al. 2018, *AJ*, 156, 123, doi: [10.3847/1538-3881/aabc4f](https://doi.org/10.3847/1538-3881/aabc4f)
- Ayres, T. R. 1997, *J. Geophys. Res.*, 102, 1641, doi: [10.1029/96JE03306](https://doi.org/10.1029/96JE03306)
- Babel, J., & Montmerle, T. 1997, *A&A*, 323, 121
- Balona, L. A. 2011, *MNRAS*, 415, 1691, doi: [10.1111/j.1365-2966.2011.18813.x](https://doi.org/10.1111/j.1365-2966.2011.18813.x)
- . 2012, *MNRAS*, 423, 3420, doi: [10.1111/j.1365-2966.2012.21135.x](https://doi.org/10.1111/j.1365-2966.2012.21135.x)
- . 2017, *MNRAS*, 467, 1830, doi: [10.1093/mnras/stx265](https://doi.org/10.1093/mnras/stx265)
- Barrado y Navascues, D. 1998, *A&A*, 339, 831, <https://arxiv.org/abs/astro-ph/9905243>
- Bell, C. P. M., Mamajek, E. E., & Naylor, T. 2015, *MNRAS*, 454, 593, doi: [10.1093/mnras/stv1981](https://doi.org/10.1093/mnras/stv1981)
- Berghoefer, T. W., Schmitt, J. H. M. M., & Cassinelli, J. P. 1996, *A&AS*, 118, 481
- Berghoefer, T. W., Schmitt, J. H. M. M., Danner, R., & Cassinelli, J. P. 1997, *A&A*, 322, 167
- Böhm, T., Holschneider, M., Lignières, F., et al. 2015, *A&A*, 577, A64, doi: [10.1051/0004-6361/201425425](https://doi.org/10.1051/0004-6361/201425425)
- Braithwaite, J. 2006, *A&A*, 449, 451, doi: [10.1051/0004-6361:20054241](https://doi.org/10.1051/0004-6361:20054241)
- Brandenburg, A., & Schmitt, D. 1998, *A&A*, 338, L55
- Brandt, G. M., Brandt, T. D., Dupuy, T. J., Li, Y., & Michalik, D. 2021, *AJ*, 161, 179, doi: [10.3847/1538-3881/abdc2e](https://doi.org/10.3847/1538-3881/abdc2e)
- Brun, A. S., & Browning, M. K. 2017, *Living Reviews in Solar Physics*, 14, 4, doi: [10.1007/s41116-017-0007-8](https://doi.org/10.1007/s41116-017-0007-8)
- Burke, D., Laurino, O., Wmclaugh, et al. 2021, *sherpa/sherpa: Sherpa 4.13.0*, 4.13.0, Zenodo, Zenodo, doi: [10.5281/zenodo.4428938](https://doi.org/10.5281/zenodo.4428938)
- Cantiello, M., & Braithwaite, J. 2019, *ApJ*, 883, 106, doi: [10.3847/1538-4357/ab3924](https://doi.org/10.3847/1538-4357/ab3924)
- Christensen-Dalsgaard, J. 2000, in *Astronomical Society of the Pacific Conference Series*, Vol. 210, Delta Scuti and Related Stars, ed. M. Breger & M. Montgomery, 187
- Cuntz, M., Rammacher, W., Ulmschneider, P., Musielak, Z. E., & Saar, S. H. 1999, *ApJ*, 522, 1053, doi: [10.1086/307689](https://doi.org/10.1086/307689)
- David, T. J., & Hillenbrand, L. A. 2015, *ApJ*, 804, 146, doi: [10.1088/0004-637X/804/2/146](https://doi.org/10.1088/0004-637X/804/2/146)
- De Rosa, R. J., Patience, J., Wilson, P. A., et al. 2014, *MNRAS*, 437, 1216, doi: [10.1093/mnras/stt1932](https://doi.org/10.1093/mnras/stt1932)
- Defrère, D., Hinz, P. M., Kennedy, G. M., et al. 2021, *AJ*, 161, 186, doi: [10.3847/1538-3881/abe3ff](https://doi.org/10.3847/1538-3881/abe3ff)
- Del Zanna, G., Dere, K. P., Young, P. R., & Landi, E. 2021, *ApJ*, 909, 38, doi: [10.3847/1538-4357/abd8ce](https://doi.org/10.3847/1538-4357/abd8ce)
- Dere, K. P., Landi, E., Mason, H. E., Monsignori Fossi, B. C., & Young, P. R. 1997, *A&AS*, 125, 149, doi: [10.1051/aas:1997368](https://doi.org/10.1051/aas:1997368)
- Doe, S., Nguyen, D., Stawarz, C., et al. 2007, in *Astronomical Society of the Pacific Conference Series*, Vol. 376, *Astronomical Data Analysis Software and Systems XVI*, ed. R. A. Shaw, F. Hill, & D. J. Bell, 543
- Drake, J. J., Braithwaite, J., Kashyap, V., Günther, H. M., & Wright, N. J. 2014, *ApJ*, 786, 136, doi: [10.1088/0004-637X/786/2/136](https://doi.org/10.1088/0004-637X/786/2/136)
- Fawzy, D., Ulmschneider, P., Stępień, K., Musielak, Z. E., & Rammacher, W. 2002, *A&A*, 386, 983, doi: [10.1051/0004-6361:20020265](https://doi.org/10.1051/0004-6361:20020265)
- Ferrero, R. F., Gouttebroze, P., Catalano, S., et al. 1995, *ApJ*, 439, 1011, doi: [10.1086/175238](https://doi.org/10.1086/175238)
- Freund, S. e. a. 2022, *subm.*
- Fruscione, A., McDowell, J. C., Allen, G. E., et al. 2006, in *Society of Photo-Optical Instrumentation Engineers (SPIE) Conference Series*, Vol. 6270, *Society of Photo-Optical Instrumentation Engineers (SPIE) Conference Series*, ed. D. R. Silva & R. E. Doxsey, 62701V, doi: [10.1117/12.671760](https://doi.org/10.1117/12.671760)
- Gaia Collaboration. 2018, *VizieR Online Data Catalog*, I/345
- Gaia Collaboration, Prusti, T., de Bruijne, J. H. J., et al. 2016, *A&A*, 595, A1, doi: [10.1051/0004-6361/201629272](https://doi.org/10.1051/0004-6361/201629272)
- Gaia Collaboration, Brown, A. G. A., Vallenari, A., et al. 2018, *A&A*, 616, A1, doi: [10.1051/0004-6361/201833051](https://doi.org/10.1051/0004-6361/201833051)
- Ginsburg, A., Sipőcz, B. M., Brasseur, C. E., et al. 2019, *AJ*, 157, 98, doi: [10.3847/1538-3881/aafc33](https://doi.org/10.3847/1538-3881/aafc33)
- Gondoin, P. 2005, *A&A*, 444, 531, doi: [10.1051/0004-6361:20053567](https://doi.org/10.1051/0004-6361:20053567)
- Gray, R. O., & Garrison, R. F. 1989, *ApJS*, 70, 623, doi: [10.1086/191349](https://doi.org/10.1086/191349)
- Gray, R. O., & Kaye, A. B. 1999, *AJ*, 118, 2993, doi: [10.1086/301134](https://doi.org/10.1086/301134)
- Günther, H. M., & Schmitt, J. H. M. M. 2009, *A&A*, 494, 1041, doi: [10.1051/0004-6361:200811007](https://doi.org/10.1051/0004-6361:200811007)

- Günther, H. M., Wolk, S. J., Drake, J. J., et al. 2012, *ApJ*, 750, 78, doi: [10.1088/0004-637X/750/1/78](https://doi.org/10.1088/0004-637X/750/1/78)
- Harris, C. R., Millman, K. J., van der Walt, S. J., et al. 2020, *Nature*, 585, 357, doi: [10.1038/s41586-020-2649-2](https://doi.org/10.1038/s41586-020-2649-2)
- Hill, G., Gulliver, A. F., & Adelman, S. J. 2010, *ApJ*, 712, 250, doi: [10.1088/0004-637X/712/1/250](https://doi.org/10.1088/0004-637X/712/1/250)
- Huélamo, N., Neuhäuser, R., Stelzer, B., Supper, R., & Zinnecker, H. 2000, *A&A*, 359, 227.
<https://arxiv.org/abs/astro-ph/0005348>
- Hunter, J. D. 2007, *Computing in Science and Engineering*, 9, 90, doi: [10.1109/MCSE.2007.55](https://doi.org/10.1109/MCSE.2007.55)
- Hurt, S. A., Quinn, S. N., Latham, D. W., et al. 2021, *AJ*, 161, 157, doi: [10.3847/1538-3881/abdec8](https://doi.org/10.3847/1538-3881/abdec8)
- Jura, M. 1991, *ApJL*, 383, L79, doi: [10.1086/186246](https://doi.org/10.1086/186246)
- Kashyap, V. L., van Dyk, D. A., Connors, A., et al. 2010, *ApJ*, 719, 900, doi: [10.1088/0004-637X/719/1/900](https://doi.org/10.1088/0004-637X/719/1/900)
- Kervella, P., Arenou, F., Mignard, F., & Thévenin, F. 2019, *A&A*, 623, A72, doi: [10.1051/0004-6361/201834371](https://doi.org/10.1051/0004-6361/201834371)
- Kupka, F., & Montgomery, M. H. 2002, *MNRAS*, 330, L6, doi: [10.1046/j.1365-8711.2002.05268.x](https://doi.org/10.1046/j.1365-8711.2002.05268.x)
- Larwood, J. D., & Kalas, P. G. 2001, *MNRAS*, 323, 402, doi: [10.1046/j.1365-8711.2001.04212.x](https://doi.org/10.1046/j.1365-8711.2001.04212.x)
- Lee, J., & Song, I. 2019, *MNRAS*, 489, 2189, doi: [10.1093/mnras/stz2290](https://doi.org/10.1093/mnras/stz2290)
- Lignières, F., Petit, P., Böhm, T., & Aurière, M. 2009, *A&A*, 500, L41, doi: [10.1051/0004-6361/200911996](https://doi.org/10.1051/0004-6361/200911996)
- Macdonald, J., & Mullan, D. J. 2010, *ApJ*, 723, 1599, doi: [10.1088/0004-637X/723/2/1599](https://doi.org/10.1088/0004-637X/723/2/1599)
- Marois, C., Macintosh, B., Barman, T., et al. 2008, *Science*, 322, 1348, doi: [10.1126/science.1166585](https://doi.org/10.1126/science.1166585)
- Meshkat, T., Mawet, D., Bryan, M. L., et al. 2017, *AJ*, 154, 245, doi: [10.3847/1538-3881/aa8e9a](https://doi.org/10.3847/1538-3881/aa8e9a)
- Monnier, J. D., Zhao, M., Pedretti, E., et al. 2007, *Science*, 317, 342, doi: [10.1126/science.1143205](https://doi.org/10.1126/science.1143205)
- Neff, J. E., & Simon, T. 2008, *ApJ*, 685, 478, doi: [10.1086/590423](https://doi.org/10.1086/590423)
- Nielsen, E. L., Liu, M. C., Wahhaj, Z., et al. 2013, *ApJ*, 776, 4, doi: [10.1088/0004-637X/776/1/4](https://doi.org/10.1088/0004-637X/776/1/4)
- Ochsenbein, F., Bauer, P., & Marcout, J. 2000, *A&AS*, 143, 23, doi: [10.1051/aas:2000169](https://doi.org/10.1051/aas:2000169)
- Pease, D. O., Drake, J. J., & Kashyap, V. L. 2006, *ApJ*, 636, 426, doi: [10.1086/497888](https://doi.org/10.1086/497888)
- Pecaut, M. J., & Mamajek, E. E. 2013, *ApJS*, 208, 9, doi: [10.1088/0067-0049/208/1/9](https://doi.org/10.1088/0067-0049/208/1/9)
- Pedersen, M. G., Antoci, V., Korhonen, H., et al. 2017, *MNRAS*, 466, 3060, doi: [10.1093/mnras/stw3226](https://doi.org/10.1093/mnras/stw3226)
- Peterson, D. M., Hummel, C. A., Pauls, T. A., et al. 2006, *ApJ*, 636, 1087, doi: [10.1086/497981](https://doi.org/10.1086/497981)
- Petit, P., Lignières, F., Wade, G. A., et al. 2010, *A&A*, 523, A41, doi: [10.1051/0004-6361/201015307](https://doi.org/10.1051/0004-6361/201015307)
- Pizzolato, N., Maggio, A., Micela, G., Sciortino, S., & Ventura, P. 2003, *A&A*, 397, 147, doi: [10.1051/0004-6361:20021560](https://doi.org/10.1051/0004-6361:20021560)
- Preibisch, T., & Feigelson, E. D. 2005, *ApJS*, 160, 390, doi: [10.1086/432094](https://doi.org/10.1086/432094)
- Primini, F. A., & Kashyap, V. L. 2014, *ApJ*, 796, 24, doi: [10.1088/0004-637X/796/1/24](https://doi.org/10.1088/0004-637X/796/1/24)
- Quanz, S. P., Kenworthy, M. A., Meyer, M. R., Girard, J. H. V., & Kasper, M. 2011, *ApJL*, 736, L32, doi: [10.1088/2041-8205/736/2/L32](https://doi.org/10.1088/2041-8205/736/2/L32)
- Robrade, J., & Schmitt, J. H. M. M. 2009, *A&A*, 497, 511, doi: [10.1051/0004-6361/200811348](https://doi.org/10.1051/0004-6361/200811348)
- . 2010, *A&A*, 516, A38, doi: [10.1051/0004-6361/201014027](https://doi.org/10.1051/0004-6361/201014027)
- . 2011, *A&A*, 531, A58, doi: [10.1051/0004-6361/201116843](https://doi.org/10.1051/0004-6361/201116843)
- Royer, F., Grenier, S., Baylac, M. O., Gómez, A. E., & Zorec, J. 2002, *A&A*, 393, 897, doi: [10.1051/0004-6361:20020943](https://doi.org/10.1051/0004-6361:20020943)
- Schmitt, J. H. M. M. 1997, *A&A*, 318, 215
- Schmitt, J. H. M. M., & Liefke, C. 2004, *A&A*, 417, 651, doi: [10.1051/0004-6361:20030495](https://doi.org/10.1051/0004-6361:20030495)
- Schrijver, C. J., & Zwaan, C. 2000, *Solar and Stellar Magnetic Activity*
- Schröder, C., & Schmitt, J. H. M. M. 2007, *A&A*, 475, 677, doi: [10.1051/0004-6361:20077429](https://doi.org/10.1051/0004-6361:20077429)
- Sikora, J., David-Uraz, A., Chowdhury, S., et al. 2019, *MNRAS*, 487, 4695, doi: [10.1093/mnras/stz1581](https://doi.org/10.1093/mnras/stz1581)
- Simon, T., Ayres, T. R., Redfield, S., & Linsky, J. L. 2002, *ApJ*, 579, 800, doi: [10.1086/342941](https://doi.org/10.1086/342941)
- Skinner, S. L., & Güdel, M. 2020, *ApJ*, 888, 15, doi: [10.3847/1538-4357/ab585c](https://doi.org/10.3847/1538-4357/ab585c)
- Skinner, S. L., Güdel, M., Audard, M., & Smith, K. 2004, *ApJ*, 614, 221, doi: [10.1086/422708](https://doi.org/10.1086/422708)
- Skrutskie, M. F., Cutri, R. M., Stiening, R., et al. 2006, *AJ*, 131, 1163, doi: [10.1086/498708](https://doi.org/10.1086/498708)
- Soubiran, C., Le Campion, J.-F., Brouillet, N., & Chemin, L. 2016, *A&A*, 591, A118, doi: [10.1051/0004-6361/201628497](https://doi.org/10.1051/0004-6361/201628497)
- Spruit, H. C. 2002, *A&A*, 381, 923, doi: [10.1051/0004-6361:20011465](https://doi.org/10.1051/0004-6361:20011465)
- Stelzer, B., Huélamo, N., Hubrig, S., Zinnecker, H., & Micela, G. 2003, *A&A*, 407, 1067, doi: [10.1051/0004-6361:20030934](https://doi.org/10.1051/0004-6361:20030934)
- Stone, J. M., Skemer, A. J., Hinz, P. M., et al. 2018, *AJ*, 156, 286, doi: [10.3847/1538-3881/aac00](https://doi.org/10.3847/1538-3881/aac00)
- Su, K. Y. L., Rieke, G. H., Misselt, K. A., et al. 2005, *ApJ*, 628, 487, doi: [10.1086/430819](https://doi.org/10.1086/430819)
- Telleschi, A., Güdel, M., Briggs, K. R., et al. 2007, *A&A*, 468, 541, doi: [10.1051/0004-6361:20065422](https://doi.org/10.1051/0004-6361:20065422)

- Tout, C. A., & Pringle, J. E. 1995, MNRAS, 272, 528, doi: [10.1093/mnras/272.3.528](https://doi.org/10.1093/mnras/272.3.528)
- van Belle, G. T. 2012, A&A Rv, 20, 51, doi: [10.1007/s00159-012-0051-2](https://doi.org/10.1007/s00159-012-0051-2)
- van Belle, G. T., Ciardi, D. R., ten Brummelaar, T., et al. 2006, ApJ, 637, 494, doi: [10.1086/498334](https://doi.org/10.1086/498334)
- Van Der Walt, S., Colbert, S. C., & Varoquaux, G. 2011, Computing in Science & Engineering, 13, 22
- van Leeuwen, F. 2007, A&A, 474, 653, doi: [10.1051/0004-6361:20078357](https://doi.org/10.1051/0004-6361:20078357)
- Vican, L. 2012, AJ, 143, 135, doi: [10.1088/0004-6256/143/6/135](https://doi.org/10.1088/0004-6256/143/6/135)
- Wang, S., Bai, Y., He, L., & Liu, J. 2020, ApJ, 902, 114, doi: [10.3847/1538-4357/abb66d](https://doi.org/10.3847/1538-4357/abb66d)
- Webb, R. A., Zuckerman, B., Platais, I., et al. 1999, ApJL, 512, L63, doi: [10.1086/311856](https://doi.org/10.1086/311856)
- Weinberger, A. J., Anglada-Escudé, G., & Boss, A. P. 2013, ApJ, 767, 96, doi: [10.1088/0004-637X/767/1/96](https://doi.org/10.1088/0004-637X/767/1/96)
- Wenger, M., Ochsenbein, F., Egret, D., et al. 2000, A&AS, 143, 9, doi: [10.1051/aas:2000332](https://doi.org/10.1051/aas:2000332)
- Wright, N. J., Drake, J. J., Mamajek, E. E., & Henry, G. W. 2011, ApJ, 743, 48, doi: [10.1088/0004-637X/743/1/48](https://doi.org/10.1088/0004-637X/743/1/48)
- Yoon, J., Peterson, D. M., Kurucz, R. L., & Zagarelli, R. J. 2010, ApJ, 708, 71, doi: [10.1088/0004-637X/708/1/71](https://doi.org/10.1088/0004-637X/708/1/71)
- Zhao, M., Monnier, J. D., Pedretti, E., et al. 2009, ApJ, 701, 209, doi: [10.1088/0004-637X/701/1/209](https://doi.org/10.1088/0004-637X/701/1/209)
- Zuckerman, B. 2019, ApJ, 870, 27, doi: [10.3847/1538-4357/aace66](https://doi.org/10.3847/1538-4357/aace66)
- Zuckerman, B., Song, I., Bessell, M. S., & Webb, R. A. 2001, ApJL, 562, L87, doi: [10.1086/337968](https://doi.org/10.1086/337968)